Distribution of total suspended solids and dynamics of the estuarine turbidity maximum in the Ipojuca River estuary

Sayonara Lins[1]*, Carmen Medeiros[1], Issac Freitas[1]

[1] Department of Oceanography – Federal University of Pernambuco (Av. Arquitetura s/n – 50740-550 – Recife – PE – Brazil).

* Corresponding author: sayonararaiza@gmail.com

ABSTRACT

This study focused on the distribution of total suspended solids (TSS) concentration along the Ipojuca River estuary and on identifying the average location of the estuarine turbidity maximum (ETM) zone considering the seasonality of its rainfall and tidal regime. This research was carried out along a 13.6 km stretch of the chosen river, with 21 sampling stations during the rainy (Jun-Jul/17) and dry periods (Dec/17). Temperature and salinity data were obtained at each station using CTD profiling. Furthermore, current intensity and direction were measured using a current meter, and water samples were collected to determine TSS concentrations. The water column showed vertically homogeneous temperature (~27° C). Salinity distribution varied seasonally and along the tidal cycle throughout the system. The estuary shows a weakly to moderately stratified water column that intensifies itself upstream. At just 2.28 km from the river mouth (second station), salinity varies by 0.2-32.9. This stratification primarily stems from the constriction of its river mouth, trapping freshwater in its interior. Currents showed higher values during the rainy period (-5 to 95.8 cms^{-1}). TSS concentrations were higher during the rainy season, ranging from 8.6 to 241.2 mg L^{-1} during spring tides and from 6.5 to 223.0 mg L^{-1} during neap tides. The ETM was located at 1.8-2.2 km from the river mouth during the rainy season and at 2-8 km during the dry season. The ETM coincided with the boundaries of salt propagation in the estuary, corresponding to salinities of 0.2-10, and longitudinal currents ranging from 60 to -10 cm s^{-1}, indicating the mixing zone of water masses. Since the ETM is also associated with the area of highest sediment deposition in the estuary, it is likely that most materials transported to the estuary that are associated with sediment transport remain trapped in this zone, making it an important area for further studies.

Keywords: Sediments, Suspended particulate matter, Constricted river mouth, Tropical estuary

INTRODUCTION

Estuaries are highly dynamic and biodiverse environments, serving as abundant sources of nourishment and refuge for aquatic organisms. The input from rivers is the primary source of materials in estuaries, which is typically associated with suspended matter in the water column (Miranda et al., 2017). Total suspended solids (TSS) consist of particles with diameters smaller than 63 μm that are dispersed throughout the water column of a water body (Millero, 2006). These particles can have both organic and inorganic origins and possess cohesive properties, causing them to adhere to one another by a process called flocculation. The flocculation of clay particles is induced by Van der Waals forces and is intensified by the detritivorous activities of microorganisms (Krone, 1962; Ye et al., 2020; 2021). In freshwater

environments with low ion concentrations, the attractive forces are relatively weaker due to the stronger repulsive forces resulting from the negatively charged grains. Conversely the positively charged sodium ions in saline waters form ionic clouds around the negatively charged clay particles, thereby accelerating the flocculation processes (Berlamont, 1993; Maggi, 2009).

In estuarine environments, TSS concentrations vary due to a range of factors, including river discharge, tidal flow, resuspension of muddy bottom deposits, tidal phase differences, estuarine longitudinal and vertical distribution mechanisms, and anthropogenic influences (Chen, 2005; Manning and Bass, 2006; Yuan et al., 2009). Within the water column, solids consist of fine sediment particles, organic matter/debris, and/or contaminants adhered to each other (Li et al., 2022). In convergence zones between freshwater and marine waters (typically characterized by low salinity), these aggregates can attract one another and other fine particles in the water, forming ensembles with larger diameters and lower densities, known as flocs. Generally, the larger the size of the floc, the lower the density and the longer the sedimentation and residence time in the water column, making them more susceptible to breakup due to turbulent movements (Gibbs, 1985; Kranenburg, 1994; Mikkelsen, 2005; Lee et al., 2012).

The distribution of TSS in an estuary varies due to tidal phase differences, lunar and solar cycles, estuarine longitudinal and vertical distribution mechanisms, and anthropogenic influences (Chen, 2005; Manning and Bass, 2006). Estuaries with limited ocean contact tend to show tidal asymmetries, resulting in longer ebbs than floods. As a result, flood tidal currents are stronger, increasing bottom shear and resuspension. The sediment accumulated in the water column begins to flocculate as the current velocity decreases, leading to the formation of clusters of TSS during low tide and flood stages. Tidal pumping can also influence TSS concentration. In the convergence zone between riverine and marine water masses (typically located near the maximum saline intrusion) during the flood stage, denser seawater is advected beneath the freshwater, causing greater turbulence. Similarly, during the ebb stage,

freshwater is advected over the denser saline water, intensifying stratification in the water column (Garel et al., 2009). This convergence area of water masses is commonly associated with the estuarine turbidity maximum (ETM) zone, defined as the peak area of TSS concentration in an estuary.

The interaction between river water carrying suspended solids toward the estuary mouth and seawater flowing upstream forms a zone with high concentrations of suspended sediments "trapped" by the advection movements of the currents. The location of this ETM zone varies depending on tidal and river discharge forces, which can shift it further upstream or downstream (Manning and Dyer, 2006; Yuan et al., 2009). Due to the influence of salinity, the speed and direction of tidal currents, and water pH on the flocculation process, the ETM is commonly associated with specific salinity values in an estuary (Ghazali et al., 2020). Several experimental and observational studies have identified critical salinities slightly above freshwater values as likely locations for the ETM, indicating variable salinities ranging by 0.5-10 (Manning and Dyer, 2002; Manning and Bass, 2006; Manning et al., 2007; Seiphoori, 2021; Krahl et al., 2022).

ETMs play a significant role in capturing and removing the particles attached to flocs in the water column, such as contaminants. The estuary serves as a major center for cycling and filtering suspended solids from rivers, enabling only a portion of these solids to reach the ocean, thereby limiting the extent of pollution due to continental waters arriving at marine ecosystems (Gibbs, 1986; Ahmerkamp et al., 2022). The studied area has few works related to ETM and TSS transport, with notable contributions from Schettini et al. (2016) in the Capibaribe River estuary, and Noriega et al. (2013) in the estuarine channel of the Port of Recife.

The overall objective of this study is to characterize the distribution of total suspended solids in the estuary of the Ipojuca river and identify its upper and lower excursion limits and the average location of its estuarine turbidity maximum zone in relation to its rainfall seasonality and tidal regime.

Study area

The Ipojuca river originates in the municipality of Arcoverde, in the semi-arid region of Pernambuco,

and spans approximately 250 km across 25 municipalities until it reaches the Atlantic Ocean, south of the Suape Industrial Complex (-8.3972° S; -34.9583° W). The drainage basin of the river is predominantly occupied by agricultural activities, with sugarcane cultivation being the most prominent (Pernambuco, 2010). Currently, the Ipojuca river ranks sixth among the most polluted rivers in Brazil (IBGE, 2017), having previously held the third position in earlier surveys (2010-2012). The main sources of pollution include pesticides, domestic sewage, and industrial effluents.

The region experiences distinct seasonal periods, with a fundamental division between September-February, characterized as the dry season, and March-August, considered the rainy season. Observations conducted over a 20-year period showed 1500 mm of precipitation during the rainy season, whereas, during the dry season, this amount fails to reach one-third of the recorded total (400 mm) (INMET, 2017). The flow of the river also varies seasonally. Based on semi-annual averages from the last 20 years, it was possible to calculate an average flow of 7.44 m^3 s^{-1} during the dry season and 27.34 m^3 s^{-1} during the rainy season. The highest average values were observed in June (with an average of 33.06 m^3 s^{-1}, reaching 84.11 m^3 s^{-1} in 2005), whereas the lowest values, in December (with an average of 5.28 m^3 s^{-1}) (ANA, 2023).

As for the estuary of the Ipojuca river, it is classified as a type 1b estuary according to Hansen and Rattray's classification and is characterized by a moderate stratification and a predominance of saline transport resulting from diffusion processes and lateral homogeneity (Lins, 2018). Near the river's mouth, in the coastal region, tides are classified as mesotidal semidiurnal, with an average spring tide amplitude of 2.0 m and an average neap tide amplitude of 0.9 m, similar to those predicted for the tide gauge station at the Port of Suape (Lins and Medeiros, 2018). The Ipojuca River connects to the Atlantic Ocean by a cut and a lowering of the reef line approximately 150 meters wide. These modifications were made during the construction of the Suape Port, resulting in the isolation of the river from its natural mouth near Cabo de Santo Agostinho. The narrow opening of the mouth of the river results in a pronounced asymmetry between flood and ebb tides, with greater oscillation during neap tides. As the tide spans the estuary of the Ipojuca river, its amplitude oscillation gradually decreases, whereas the asymmetry between flood and ebb tides becomes more evident.

METHODS

Data sampling was comprehensively conducted to cover both the rainy (Jun-Jul/17) and dry seasons (Dec/17), representing various tidal cycle stages (low tide, flood, high tide, and ebb) during spring and neap tides in 2017. Overall, five strategically chosen stations were established within the estuary. Station 1 was located near the river mouth, Station 2 was positioned just upstream of the estuary basin, Station 3 was situated downstream from the main channel bifurcation, and Stations 4 and 5 were positioned within the internal meanders of the river. Station 5 was specifically selected to represent the fluvial water (Figure 1). Refinement points were distributed across the stations to precisely determine the location of the maximum turbidity zone during the rainy (R01-R12) and dry periods (R13-R16) (Table 1).

Table 1. Geographical location and average depth of the main (1-5) and refinement stations (R01-R16) in the Ipojuca river estuary.

Station	UTM E (25S)	UTM N (25S)	LAT. (°S)	LONG. (°W)	Average depth
1	283214	9069779	-8.410466779	-34.96886597	6.40
2	281641	9069908	-8.409228871	-34.98314029	2.40
3	276937	9069750	-8.410565005	-35.00134041	4.80
4	277535	9068167	-8.424777279	-35.02049693	6.03
5	275906	9069443	-8.413166327	-35.03522538	5.15
R1	282624	9070195	-8.406679298	-34.97420317	2.65
R2	282416	9070560	-8.403370232	-34.97607474	2.90
R3	282391	9070364	-8.405140925	-34.97631067	1.50
R4	282141	9070262	-8.406051593	-34.97858491	1.75
R5	282031	9070054	-8.407926877	-34.97959305	1.05
R6	281900	9069855	-8.409719837	-34.98079145	0.85
R7	281210	9069731	-8.410809183	-34.98706118	1.05
R8	280939	9069761	-8.410525547	-34.98952002	2.35
R9	280729	9069837	-8.409828866	-34.99142295	1.75
R10	280530	9069736	-8.410732740	-34.99323419	2.05
R11	280297	9069687	-8.411164965	-34.99535169	2.50
R12	280119	9069776	-8.410352215	-34.99696350	2.40
R13	279313	9069638	-8.411562482	-35.00428696	1.50
R14	278817	9069187	-8.415616441	-35.00881076	3.30
R15	278441	9068812	-8.418988885	-35.01224171	2.15
R16	277986	9068164	-8.424825449	-35.01640269	1.68
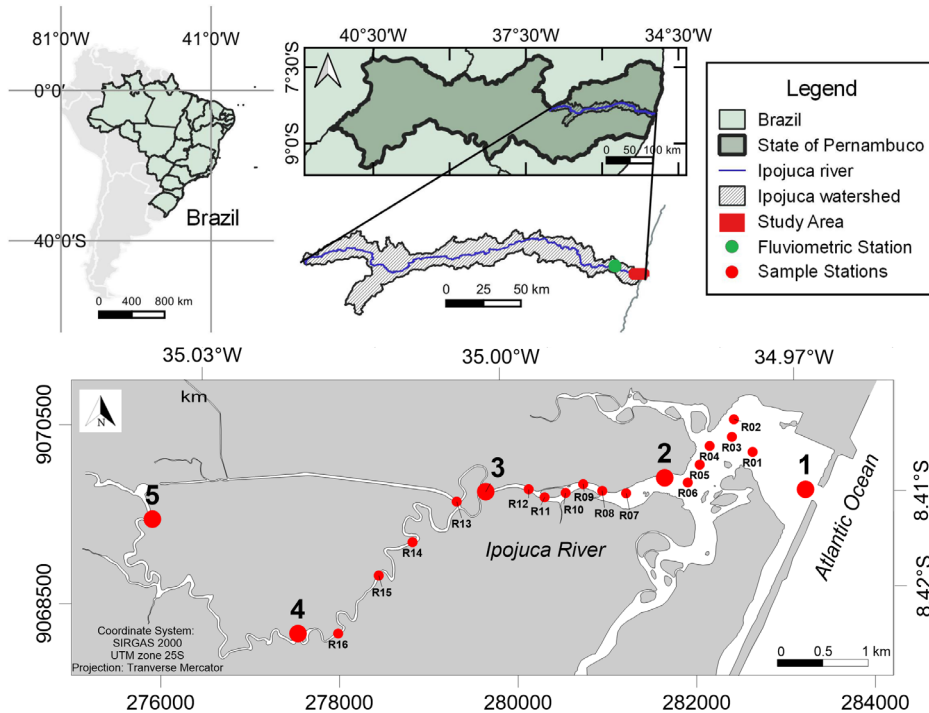
Figure 1. Location of the estuarine section of the Ipojuca River, indicating the main sampling stations 1-5 with a large red circle, and refinement stations R01-R16 with smaller red circles. Source: IBGE, 2021 (Brazil and Hydrographic Basin); Author, 2023 (Estuary Limits of the Ipojuca River).

To characterize the rainfall regime and river inflows for the study area, air temperature and rainfall data were compiled from the meteorological station at the Port of Suape (-8.3972° S; -34.9583° W), provided by the Water and Climate Agency of Pernambuco (Agência Pernambucana de Águas e Climas – APAC), whereas river flow values for the Ipojuca river were obtained at the fluviometric station 39370100 (-8.3697° S; -35.1422° W), accessed by the National Water Agency (Agência Nacional de águas – ANA).

During the rainy season, when salinity is primarily confined to areas near the river mouth and the ETM is commonly linked with salinity 4, refinement points R01 to R12 were conducted. Meanwhile, refinement points R13 to R16 were conducted during the dry season.

Continuous vertical profiles of temperature and salinity were obtained from the surface to the bottom using a Sea-Bird Electronics SBE19Plus CTD profiler. The CTD profiler operated at a sampling rate of 4 Hz and was equipped with sensors for conductivity (resolution = 0.00005 sm⁻¹), temperature (resolution = 0.0001 °C), and pressure

(resolution = 0.010 m), powered by a SBE 5T centrifugal pump. The calculation of physical properties was performed using the software provided by the manufacturers of the equipment following TEOS-10 specifications (IOC et al., 2010).

For more accurate and reliable measurements, descending CTD data were used, in a manner so the turbulence caused by the equipment would fail to influence the collected data. To remove spurious data (collected in the atmosphere, at the wind-influenced surface), the first 10 centimeters of the water column were removed from the profiles. Subsequently, the data were referenced in space and time to create the graphs.

Water samples were collected at the surface, mid-depth, and bottom using a Van Dorn Horizontal water sampler, whereas measurements of current intensity and direction were taken at the surface, mid-depth, and bottom using a Sensordata SD30 current meter.

In the laboratory, water samples were vacuum-filtered through acetate and cellulose nitrate membranes with a nominal pore size of 0.45 µm and a diameter of 47 mm. Prior to filtration, the membranes

were dried in an oven (60 °C) and weighed using an analytical balance. The concentration of TSS was determined by calculating the difference in dry weights of the filters before and after filtration, relative to the filtered volume (Strickland and Parsons, 1972).

The current data were corrected for magnetic declination and decomposed into longitudinal and transverse components to the sampling sections. Along the longitudinal axis of the section, positive values indicate downstream estuarine currents, whereas negative values indicate upstream estuarine currents (Miranda, 2017).

Recognizing that salinity data within the estuary show phase differences due to "salt trapping" (Lins and Medeiros, 2018), salinity data were phase-corrected in values between 1.5-2 h, as observed in the study by Lins (2018). Subsequently, uniform grids of horizontal distributions for salinity, TSS and currents were generated by interpolating the corrected data using the Kriging method, taking into consideration the spatial variability of the measurements. This approach allowed for the creation of smooth and continuous maps and providing a comprehensive understanding of their spatial patterns within the study area.

Statistical analysis

Descriptive (mean, standard deviation, median, minimum, and maximum) and non-parametric statistics (Mann-Whitney, Kruskal-Wallis, and Dunn's tests) of the obtained results were calculated using the mStatGraph 1.5 software, developed by Varona et al. (2023). This software enabled the comprehensive analysis and interpretation of the data, providing valuable insights into the statistical properties and significant differences of the study findings. Non-parametric statistical analyses were applied to the obtained temporal data (TSS, salinity, and rainfall) to identify statistically significant differences (Mann-Whitney test; $p < 0.05$) between climatic sessions (rainy and dry periods), tidal stages (flood and ebb), and surface and bottom. Additionally, the sampling points (N = 5) were statistically analyzed for TSS and salinity using the non-parametric Kruskal-Wallis test ($p < 0.05$), followed by the Dunn's test to identify significant differences between these points.

RESULTS

Rainfall and fluvial discharge

The studied year (2017) showed a strong seasonality of its rainfall regime, with a rainy period (May to August) with great precipitation and a dry period (January-February and November-December) with reduced precipitation according to the statistical analysis between the historical rainfall (20 years) and the studied period, showing no significant differences between the historical and study periods (Mann Whitney test; $p = 0.7$; $\alpha = 0.05$) and representing the reality of the estuary well.
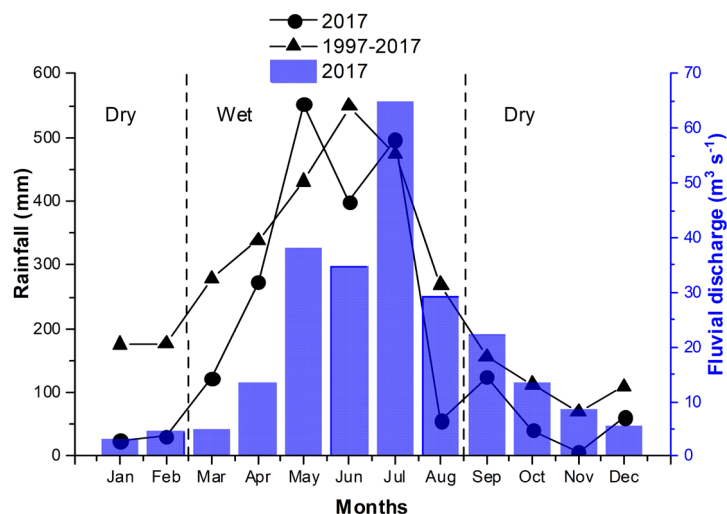
Figure 2. Fluvial discharge at the Eng. Maranhão fluviometric station (bars) and rainfall of the meteorological station at the Port of Suape (black lines) in the Ipojuca River estuary in 2017 compared to the 10-year historical average (1997 to 2017). Dashed lines indicate the climatic periods, wet = wet period; dry = dry period.

During 2017, the flow of the Ipojuca River at the Eng. Maranhão fluviometric station (Figure 1 and Figure 2), varied from 6.0 to 300.0 m^3 s^{-1} (mean = 20.3 ± 18 m^3 s^{-1}), following the rainfall regime of the region. Statistical analysis between the historical period (20 years) and the study period showed no significant differences (Mann Whitney test; p = 0.8; ∝ = 0.05).

TEMPORAL AND SPATIAL STATISTICS OF TSS AND SALINITY

Statistical results for TSS (p = 0.0001) and salinity (p = 0.0001) showed significant differences (Mann-Whitney test; p < 0.05; α = 0.05) between the observed climatic periods

(Table 2). TSS concentrations during the wet period were approximately 3.5 times higher than those observed during the dry period (mean wet period = 69 ± 40 mg L^{-1}; mean dry period = 20 ± 1 mg L^{-1}).

Salinity showed no large differences in mean values between climatic periods (mean wet period = 7.4 ± 1; mean dry period = 6.4 ± 0.9).

Significant differences were also observed in TSS concentrations (p = 0.01) between the spring and neap periods (Mann-Whitney test; p < 0.05; α = 0.05). In these periods, salinity showed no statistically significant differences (p = 0.19), ranging from 6.5 ± 1.1 (mean) at neap to 7.2 ± 0.9 (mean) at spring.

Table 2. Temporal and spatial statistics in the Ipojuca River estuary. **KW**: Kruskal-Wallis test; **MW**: Mann-Whitney test. p < 0.05 indicates significant differences for α = 0.05. In bold, significant p-values. st indicates the sampling points. Dunn's test was used after the KW test for different combinations of data sets (stations).

Parameter\tests	MW test (rainy/dry)	MW test (spring/neap)	MW test (surface/bottom)	MW test (flood/ebb)	KW test (Stations)	Dunn test (st.1/st.2/st.3/st.4/st.5)
TSS (mgL^{-1})	p = 0.0001	p = 0.01	p = 0.76	p = 0.08	p = 0.0005	st.1 ≠ st. 2; p = 0.0006 st.1 ≠ st. 3; p = 0.0009 st.1 ≠ st. 4; p = 0.0006 st.1 ≠ st. 5; p = 0.0005
Salinity	p = 0.0001	p = 0.19	p = 0.11	p = 0.47	p = 0.0009	st.1 ≠ st. 3; p = 0.002 st.1 ≠ st. 4; p = 0.0001 st.1 ≠ st. 5; p = 0.00004 st.2 ≠ st. 4; p = 0.0003 st.2 ≠ st. 5; p = 0.0009 st.3 ≠ st. 4; p = 0.0001 st.3 ≠ st. 5; p = 0.0006

In the ebb and flood stages, no significant differences were observed (Mann-Whitney test; p > 0.05; α = 0.05) for TSS (p = 0.08) and salinity (p = 0.47), respectively. TSS showed close mean values (flood = 46.8 ± 4.6 mg L^{-1}; ebb = 40.3 ± 4.9 mg L^{-1}), whereas salinity ranged from 5.2 ± 1.2 (flood) to 7.5 ± 1.4, respectively.

The spatial statistical results of this study for TSS and salinity showed no significant differences (Mann-Whitney test; p > 0.05; α = 0.05) for the surface and bottom samples (Table 2). The mean value for TSS at the surface totaled 41.3 ± 3 mg L^{-1}, whereas, at the bottom, the mean value totaled 45.0 ± 4 mg L^{-1}.

Similar to TSS, salinity had a higher mean value at the bottom of the water column (9.2 ± 1.1 units); whereas, at the bottom, the mean value was 4.5 ± 0.7 units.

The sampling stations were statistically analyzed using the Kruskal-Wallis (α = 0.05) and Dunn's tests (comparative analysis).

TSS showed significant differences for the five analyzed stations (p = 0.0005), whereas the Dunn's test showed that station 1 differed from the remaining ones (Table 2). The mean values of the studied stations showed increasing values from st.1 to st.5 (12.2 ± 2.1 mg L^{-1}; 40.6 ± 6.8 mg L^{-1}; 46.3 ± 5.5 mg L^{-1}; 64.4 ± 10.7 mg L^{-1}, and 76.7 ± 11.2 mg L^{-1}, respectively).

Salinity (p = 0.0009) showed significant differences (Kruskal-Wallis; p < 0.05; α = 0.05) for the sampling stations. The results observed through Dunn's test showed stations 4 and 5 different from the other 3 (stations 1, 2 and 3). These stations (4 and 5) had typical freshwater mean values (salinity < 0.5 units). Thus, the

sequence from station 1 to 5 was 26.8 ± 2.0; 12.7 ± 2.3; 7.1 ± 1.9; 0.1 ± 0.007; 0.1 ± 0.01, respectively.

TEMPERATURE, SALINITY, AND CURRENTS

TSS, salinity, and current data are tabulated in supplementary material Table S1. Along the water column, temperature values were homogeneous for all sampling stations. Values ranged from 23-27 °C to 26-34 °C during the wet and dry seasons,

respectively (Figure 3A). Salinity was moderately stratified along the profiles, intensifying upstream of the river and with great differentiation between tidal stages for the two studied periods but without statistically significant differences. The highest values were observed near the mouth of the estuary, decreasing upstream of the river, and never reaching station 5. The longitudinal variation of salinity changed seasonally along the tidal cycle (Figure 3B).
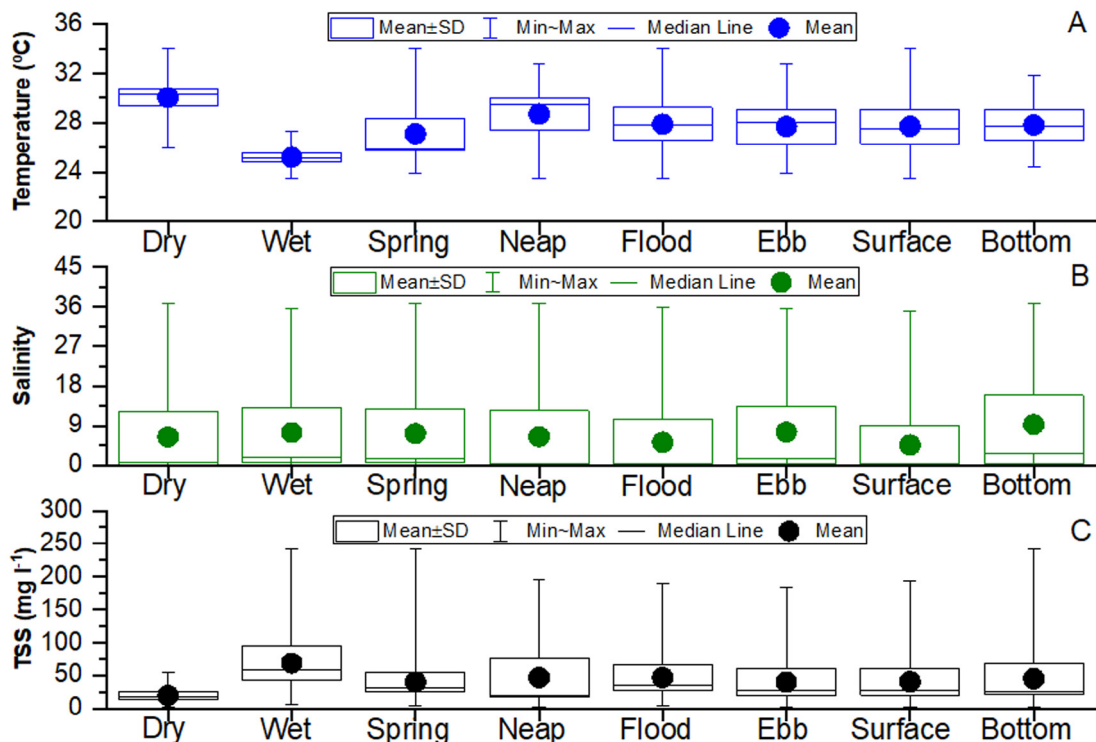
Figure 3. Temporal and spatial variations of temperature (A), salinity (B), and TSS (C) in the Ipojuca River estuary during 2017.

During the rainy season, the maximum salinity limit varied from 700 m upstream of the first station (flood stage) to 1 km upstream of the third station (ebb stage), covering a penetration distance of 5.4 km (Figure S1A). Near the mouth of the river, at station 1, salinity ranged from 2 to 35 and from 5.3 to 35.8 for spring and neap tides, respectively (Figure S1A). Further inland, the stratification becomes more intense, with salinity variations from 0.2 to 35.3 and from 0.4 to 31.8 for spring and neap tides, respectively, at station 2. At station 3, no more salinity is found at the surface, only a saline wedge is found near the bottom, ranging

from 0.1 to 30.4 and from 0.1 to 0.7 for spring and neap tides, respectively. During the dry season (Figure S1B), salinity was always observed upstream of station 3 in all tidal cycles, with maximum penetration at 6.7 km from the mouth of the estuary. Considering the same sampling stations, salinity values corresponding to the dry season ranged from 20.1 to 36.9 and from 13.8 to 36.8 at station 1, from 4 to 34.4 and from 1.7 to 32.9 at station 2, and from 0.2 to 27.8 and from 0.1 to 26.9 at station 3, for the spring and neap tides, respectively; showing a similar distribution to that observed in the other period (Figure S1B).

The values of the longitudinal velocity component u ranged from -14.3 to 89.2 cm s^{-1} for the spring tide and from -5 to 95.8 cm s^{-1} for the quadrature tide of the wet season (Figure S1A); and from -15.9 to 51.3 cm s^{-1} for the spring tide and from -17.2 to 39.1 cm s^{-1} for the neap tide of the dry season (Figure S1B). Currents were most intense at the surface during the wet season (Figure S1A).

Estuarine current velocity (*u*) components showed a predominance of longitudinally positive values for the wet and dry periods, indicating flushing flow. In general, lower values of *u* were obtained at the stations near the mouth of the estuary, near the bottom, and in the area in which the water masses meet.

TSS VARIATIONS

TSS concentrations ranged from 8.6 to 241.2 mg L^{-1} and from 6.5 to 223.0 mg L^{-1}, respectively, for the spring and neap tides during the wet season, and from 3.67 to 55.7 mg L^{-1} and from 2.45 to 55.13 mg L^{-1} respectively, for the spring and neap tides during the dry season (Figure 3C, Figure 4 to Figure 7).

TSS concentrations varied seasonally and over the tidal cycle, with high values mainly in the wet period during neap and in the low-water (LW) and flood (FW) stages (Figure 3 and 7). The dry season (Figure 6 and 7) had much lower TSS concentrations than the wet season (< 55.7 mg L^{-1}), with the highest TSS concentrations during the low-water and flood stages for both tides (spring and neap). The lowest concentrations were observed near the mouth of the estuary, increasing upstream to a peak near station 2 and/ or 3 for the wet season, and reaching stations R01 and R02 during some tidal stages during the dry season. The location of the TSS peaks corresponded to the regions of salinities close to 0.5-10 values, the limit of the saline wedge. After peak concentration, TSS values decrease to an average value of 18 mg L^{-1} and increase again upstream of the river. Due to the main channel being the major source of TSS to the inner estuary, high concentration values were found between stations 4 and 5, corresponding to river discharge (Figure 5).
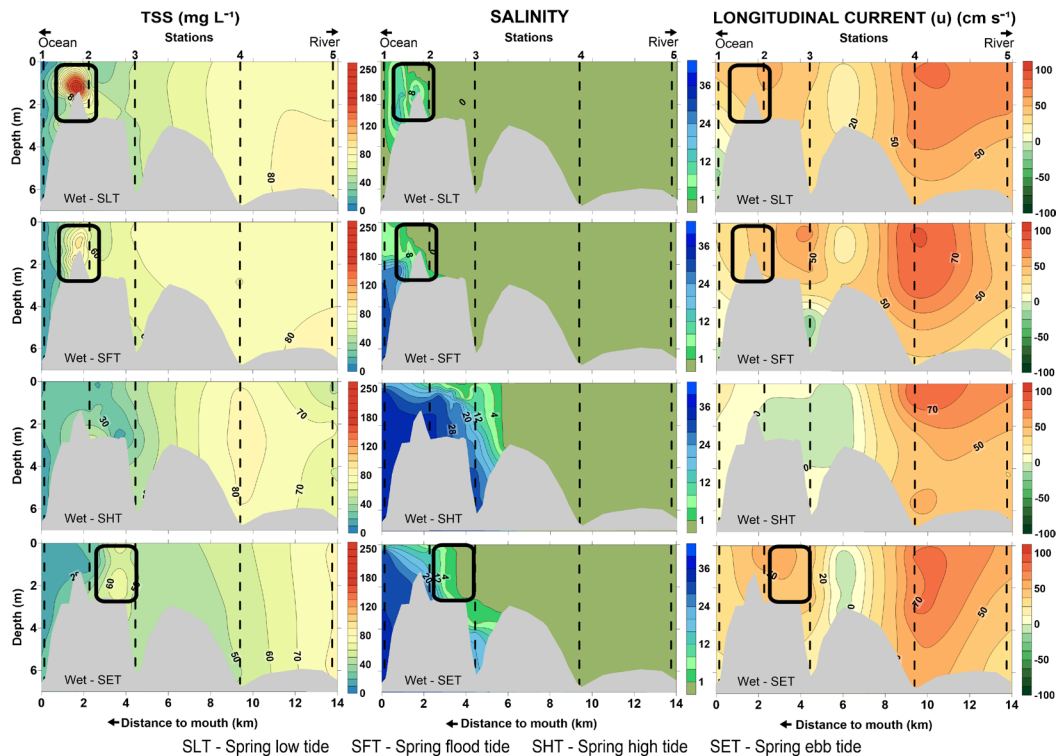
Figure 4. Location of the Estuarine Turbidity Maximum Zone (mgL^{-1}) in relation to TSS concentration, salinity, and longitudinal currents (cm s^{-1}) along the Ipojuca River estuary during the wet season of spring tides during a tidal cycle: low tide (SLT), flood (SFT), high tide (SHT), and ebb (SET).
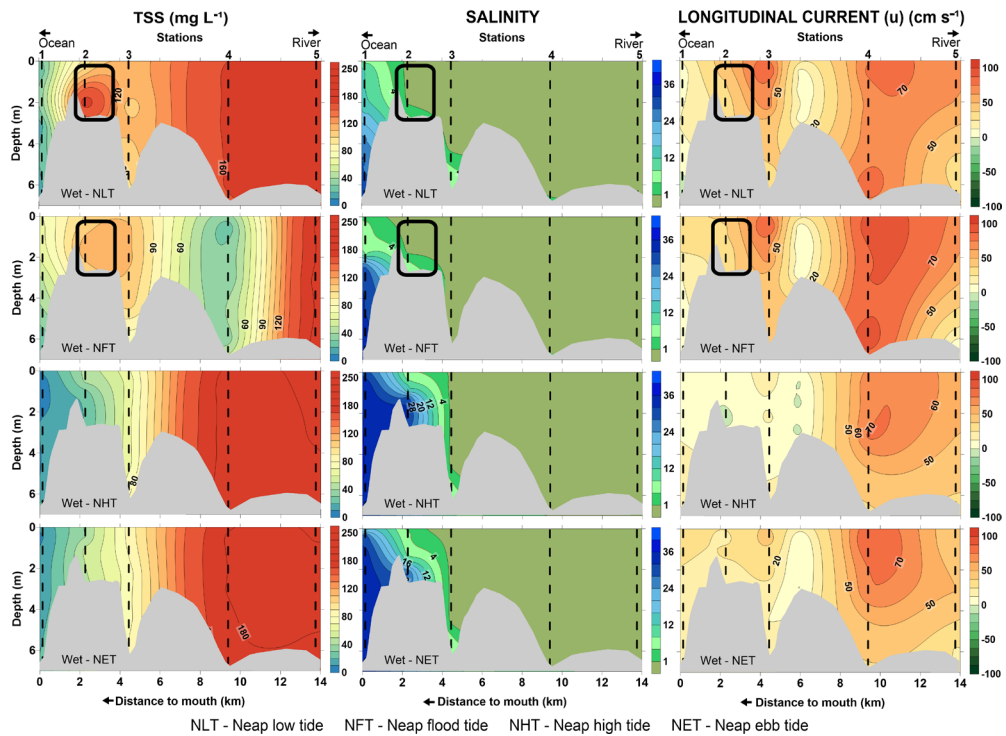
Figure 5. Location of the Estuarine Turbidity Maximum Zone (mg L⁻¹) in relation to TSS concentration, salinity, and longitudinal currents (cm s⁻¹) along the Ipojuca River estuary during the wet season of neap tides during a tidal cycle: low tide (NLT), flood (NFT), high tide (NHT), and ebb (NET).
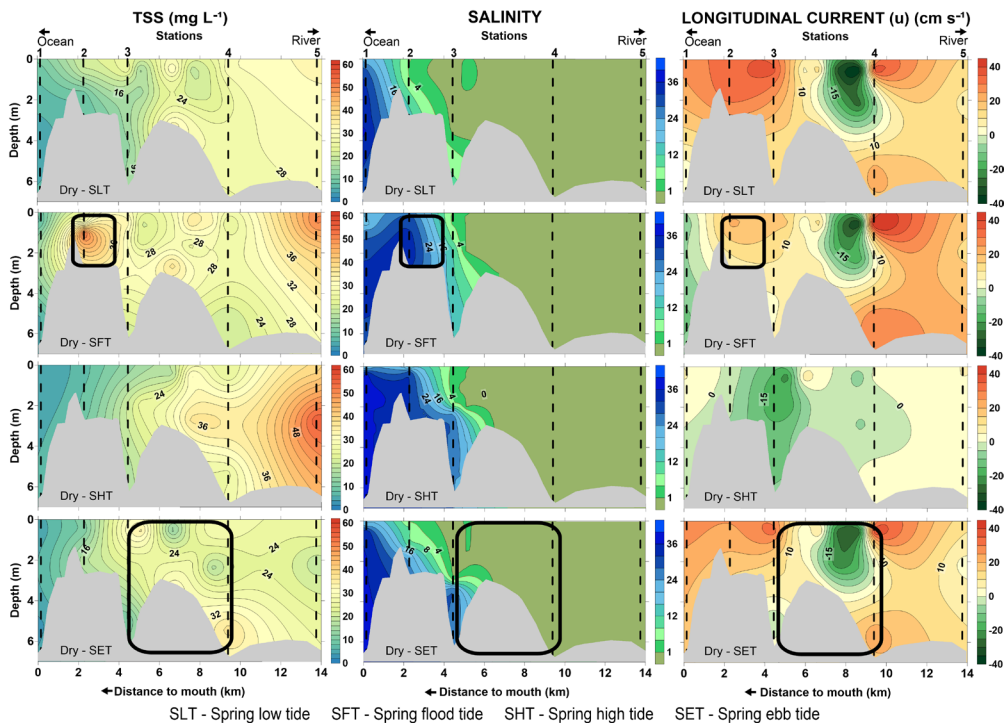
Figure 6. Location of the Estuarine Turbidity Maximum Zone (mgL⁻¹) in relation to TSS concentration, salinity, and longitudinal currents (cm s⁻¹) along the Ipojuca River estuary during the dry season of spring tides during a tidal cycle: low tide (SLT), flood (SFT), high tide (SHT), and ebb (SET).
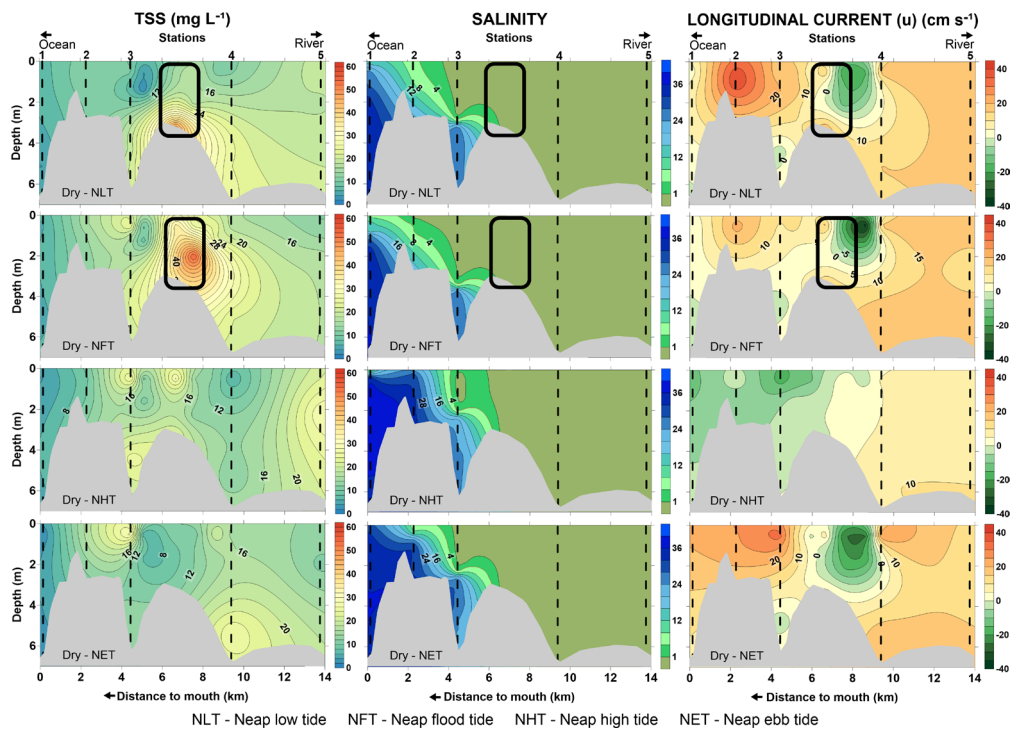
Figure 7. Location of the Estuarine Turbidity Maximum Zone (mg L⁻¹) in relation to TSS concentration, salinity, and longitudinal currents (cm s⁻¹) along the Ipojuca River estuary during the dry season of neap tides during a tidal cycle: low tide (NLT), flood (NFT), high tide (NHT), and ebb (NET).

Estuarine turbidity maximum (ETM)

The ETM, located at the peaks of TSS concentration in the intermediate region (low salinity) of the estuary, varied seasonally and between each tidal stage and may temporarily disappear in the calmest stages.

In the wet season, the ETM was located near stations R05 (241.2 mg L⁻¹ on the bottom and 66.3 mg L⁻¹ on the surface) and R04-R06 (97.9, 100.5, and 92.9 mg L⁻¹ near the bottom, respectively) for low and flood tides during spring and neap tides, respectively. During the high tide, the ETM was located near station R08 at the bottom (46.4 mg L⁻¹), whereas, during the ebb, the ETM was located at station R10, with 63.4 and 63.7 mg L⁻¹ at the surface and bottom, respectively (Figure 4 and 5).

In the dry season (Figure 6 and 7), the migration distance of the ETM between tidal stages was distinct between the different tidal types, with the largest excursion during the spring tide and the smallest during the neap tide. In the spring tide (Figure 6), the ETM was located between stations

2 and 3 during the flood and after station 3 during the remaining stages of the tidal cycle (R14-R15). The excursion of the ETM was more internal to the river during the high tide stage (32.3 and 36.6 mg L⁻¹ for surface and bottom, respectively).

In the neap period (Figure 7), high TSS concentrations were observed in the vicinity of station 3 (flood, high tide, and ebb) with 24.3; 22.6; 26.6; 25.0; 29.2, and 13.1 mg L⁻¹ TSS concentrations at surface and bottom, respectively), but an ETM is located in the vicinity of station R14 only during the low tide and flood (15.0 and 49.1 mg L⁻¹ for surface and bottom, respectively).

DISCUSSION

Being a shallow tropical estuary, temperature was generally homogeneous throughout the water column, varying little during the tidal cycle of the wet season. In the dry season, during the spring tide, a greater variation of the mean temperature values along the tidal cycle was observed due to the high solar incidence (mean temperature/December: 28.1 °C) and low precipitation (precipitation/

December: 50 mm), obtaining lower values in the tidal stages occurring in the early and late hours of the day. This variation in solar intensity during the day is little evidenced during rainy cloudy days. Additionally, 2017 was characterized as a typical normal year, with little rainfall during the summer months and abundant rainfall volumes in winter, in which 74% of the annual total occurred from May to July (Lins and Medeiros, 2018).

Overall, an estuary tends to exhibit lower salinity and high TSS concentrations during the wet season, especially in the low tide stages due to the greater fluvial influence and lower tidal range in the estuarine interior; and show high salinity values and low TSS concentration during dry periods, especially in the high tide stage (Talley et al., 2011). Non-parametric statistics (Mann-Whitney test; $p < 0.05$) showed significant differences between the two climatic periods. This behavior is partially observed for the Ipojuca River estuary. The highest TSS concentrations were reached during the wet season due to the large amount of river discharge in the estuary, with averages of 50.3 and 98.4 mg L^{-1} for the spring and neap tides, respectively. The lowest concentrations were obtained during the dry period, in which the flow of the Ipojuca River was lower (mean/Dec = 5.7 m^3 s^{-1}), with mean values of 23.5 and 14.8 mg L^{-1} for the spring and neap periods, respectively (Figure 3C). However, due to the large tidal asymmetry of the Ipojuca River estuary, the highest TSS concentrations are observed in the low-water and flood stages during the wet period and in the flood and ebb stages during the dry season. The asymmetry is more subtle during the neap tide as the tidal influence is weaker since this phenomenon is caused by forces contrary to the tidal movement, such as river input, friction during the inflow, and difficulty w ith t he outflow during the exit of the tide from the estuary. This was also observed by Asp et al. (2012) in an Amazon estuary; in which the asymmetry of the tides that favor the flood currents causes the absence of an effective river discharge.

Higher salinity values were found in the ebb stages of the spring tide and in the ebb tide stages during the neap tide for the rainy season. In the dry period, due to the smaller phase difference, the highest salt concentrations were also observed

in the ebb and flood stages. The estuary was moderately stratified. This stratification was more intense during the wet period due to the higher flow of the Ipojuca River.

In an open estuary, the presence of this type of asymmetry (higher ebb times) is usually associated with greater sediment import due to greater fluvial strength against the tides, resulting in cleaner waters (Miranda et al., 2017); However, as the asymmetry found in the Ipojuca estuary is caused by the constriction of the mouth, this phenomenon actually indicates the difficulty of the waters to leave the estuary, making the waters more turbid and enabling the sediment in the water column to decay and silt the channel of the middle and lower estuary.

According to Barcellos and Santos (2018), the modification of the mouth of the Ipojuca estuary was carried out for the implementation of an industrial complex that began in the 1980s, which subsequently underwent other changes that resulted in the geomorphological alteration of the Ipojuca River mouth region.

The zone of maximum turbidity (ETM) can change in size and migrate longitudinally depending on the physical, chemical, and biological factors of the estuary. The flocculation process is mainly related to the concentration of suspended solids and the salinity of the water but it is also related to the velocity of the currents and biotic activities (biofilms) (Krahl, 2022). In partially-highly stratified estuaries, tidal pumping and current velocity are decisive in the formation of ETM, and this process is more intense during flood stages than during ebb stages (Garel, 2009). Moreover, the increase in current velocity causes flocs to remain longer in the water column and resuspend bottom sediments.

Low salinity values coincided with the location of TSS concentration peaks in the Ipojuca River estuary. When comparing TSS concentration, salinity, and current velocity for spring and neap tides in the rainy and dry periods, it is possible to observe a correlation between these three variables. Note that the ETM is greater with the increase in current speeds and/or when the estuarine and river water masses meet, in addition to being shifted downstream during periods of high river flow, which, in the case of Ipojuca, due to tidal

asymmetry, is during the flood stage. Also, the ETM of the Ipojuca River estuary coincided with the limit of saline intrusion, with salinities varying from 0.1 to 10 units, being more intense during the highest current velocities (Figures 4 to 7).

During the wet period (spring and neap), the ETM was located 1.8 and 2.2 km from the mouth in the low tide and flood stages, respectively. During the ebb stage, the ETM was located 3.5 km from the mouth (TSS = 60 mg L^{-1}). In the dry period (spring tide), the ETM was located 2.2 km from the mouth during the flood (TSS = 50 mg L^{-1}) and at 5-10 km in the ebb stage (TSS = 36 mg L^{-1}). During the neap tide, the ETM was identified 6.5 km from the mouth at low tide (TSS = 44 mg L^{-1}) and 7.8 km during the flood (TSS = 52mg L^{-1}).

Similar results were found for the Capibaribe River estuary, noting that the formation of the ETM in the estuary was associated with low salinities in the mixing zone (Schettini, 2016). Similarly, in the Weser estuary, the ETM was also formed associated with the mixing zone, at 2-10 salinities, and being the area of greatest sedimentary deposition (Köster, 2014).

A study of the sand fractions of the Ipojuca River estuary (Veiga, 2021) determined a greater continental influence on the sedimentation of the estuarine-lagoon environment, typical of transport by river input and subaqueous reworking. In that study, the continental influence was greater on the left bank of the meanders, corroborating the preferential direction of estuarine currents and sediment accumulation observed in this study, in addition to showing that the origins of these sediments were fluvial, transported by the water column or along the bottom (Veiga, 2021).

Estuarine sediments, especially those with low energy, actively depend on suspended solids brought by the river (Baptista Neto et al., 2004). Near station 2, the highest concentration of TSS was also influenced by the fluvial input of the Merepe River to the estuarine system. Miranda (2019) analyzed the chemical characteristics of water and its relation with TSS for the Merepe River and the estuarine area, observing TSS values that ranged from 0.2 to 10.8 mg L^{-1}, showing the highest values upstream. The Merepe River is a

point of less influence of TSS to the estuary when compared to the Ipojuca River.

Miranda (2019) even studied the correlations between nutrients and TSS, finding a moderate positive correlation between total chlorophyll a and TSS (31%) and a negative correlation between N-nitrate and TSS (-38%). We can therefore state that the higher concentration of TSS in the Ipojuca River estuary contributes to a higher concentration of nutrients in the area. However, its high turbidity prevents the penetration of light into the water column, reducing the production of oxygen by phytoplankton and promoting the consumption of dissolved oxygen by the processes of mineralization of the organic matter in the fine sediments by bacteria. Batista and Flores-Montes (2014) confirmed the strong anthropic impact on the Ipojuca River estuary. They analyzed the high loads of nutrients, such as nitrogen and phosphorus, reaching 535.6 μg L^{-1} in the raining season, in addition to low values of dissolved oxygen, a sign of high decomposition activity and resulting in poor water quality.

Studies on the ETM are especially important in the analysis of the associated biota and pollutants. The variation in salinity and turbidity directly influences the distribution of biota in estuaries (Telesh and Khlebovich, 2010; Turner and Millward, 2022), with the alteration of these variables being more intense longitudinally in shallow estuaries, as is the case of Ipojuca. The ETM shows greater biodiversity in the estuary, with the interaction between freshwater and marine species.

Studies on concentrations of polycyclic aromatic hydrocarbons (PAHs), a highly carcinogenic substance related the particulate matter in suspension with the concentration of this pollutant find the accumulation of this pollutant in the ETM (Arruda et al, 2018), thus evincing the importance of studying the distribution of TSS and estuarine currents for the preferential zones of sedimentary deposition.

CONCLUSION

The temperature was homogeneous throughout the water column, characteristic of a shallow tropical estuary. The distribution of TSS between the two studied periods differed, with the concentration

being 3.45 times higher in the wet period than in the dry season due to greater river input.

Salinity was moderately stratified along the profiles, intensifying upstream of the river and with great differentiation between tidal stages for the two studied periods. Currents were most intense at the surface and during the wet season.

Because it is a strangulated estuary with tidal asymmetry, in which the period of the real ebb stage is longer than that predicted for the outer area of the estuary, the highest TSS concentrations were observed not only in the low-water stage but also in the flood stage, which would still correspond to the low-water stage in the inner estuary.

The ETM coincided with the location of the mixing zone between river and ocean water. A longitudinal flow change and low salinity values (0.5–10) were also observed as the ETM was displaced downstream during periods of high river flow. The ETM could be observed during flood and low tides, with greater fluvial influence, higher current velocities, and resuspension of bottom sediments. During the wet period, the ETM was located at 1.8 and 2.2 km from the mouth during spring tides and neap tides, respectively; whereas, during the dry period, the ETM varied from 2 to 10 km for spring tides and from 6.5 to 7.8 km from the mouth for neap tides.

As the ETM is also associated with the area of greatest sediment deposition in the estuary, it is possible that much of the TSS coming from the Ipojuca River, including the presence of pollutants, remains trapped in this region of the estuary, mainly due to the difficult flow of water, silting the estuarine channel. The understanding of this sedimentation process is necessary to plan management and dredging in the area.

ACKNOWLEDGMENTS

AUTHOR CONTRIBUTIONS

S.R.R.M.L.: Conceptualization; Investigation; Writing – original draft; Writing – review & editing.

C.M.: Conceptualization; Supervision; Project Administration; Writing – review & editing.

I.C.F.: Methodology; Logistics; Formal Analysis; Investigation; Writing – review & editing.

REFERENCES

Ahmerkamp, S., Liu, B., Kindler, K., Maerz, J., Stocker, R., Kuypers, M. M. M. & Khalil, A. 2022. Settling of highly porous and impermeable particles in linear stratification: Implications for marine aggregates. *Journal of Fluid Mechanics*, 931, A9. DOI: https://doi.org/10.1017/jfm.2021.913

ANA (National Water Agency). 2023. *HIDROWEB: Hydrometeorological Database*. v3.2.7. Available from: https://www.snirh.gov.br/hidroweb/apresentacao. Access on: 2023 Oct. 20.

APAC (Pernambuco Agency of Waters and Climate). 2022. *Rainfall Station Data*. Available from: http://old.apac.pe.gov.br/meteorologia/monitoramento-pluvio.php. Access on: 2022 July 15.

Arruda-Santos, R. H., Schettini, C. A. F., Yogui, G. T., Maciel, D. C. & Zanardi-Lamardo, E. 2018. Sources and distribution of aromatic hydrocarbons in a tropical marine protected area estuary under influence of sugarcane cultivation. *Science of the Total Environment*, 624, 935-944. DOI: https://doi.org/10.1016/j.scitotenv.2017.12.174

Asp, N. E., Schettini, C. A. F., Siegle, E., Silva, M. S. & Brito, R. N. 2012. The dynamics of a frictionally-dominated Amazonian estuary. *Brazilian Journal of Oceanography*, 60(3), 391-403. Available from: https://www.scielo.br/j/bjoce/a/4BLrPPhmJVrk75ytLNk7TgR/?lang=en. Access on: 2024 May. 16.

Barcellos, R. L. & Santos, L. D. 2018. Histórico de impactos e o estado da arte em Oceanografia no sistema estuarino-lagunar de Suape-Ipojuca (PE). *Parcerias Estratégicas*, 26(46), 155-168. Available from: https://seer.cgee.org.br/parcerias_estrategicas/issue/view/86. Access on: 2024 May. 16.

Baptista Neto, J. A., Abelin, V. R. P. & Sichel, S. E. 2004. Introdução à Geologia Marinha. Rio de Janeiro, Interciência.

Batista, T. N. F. & Flores-Montes, M. J. 2014. Estado trófico dos estuários dos rios Ipojuca e Merepe – PE. *Tropical Oceanography*, 42(3), 22-30. DOI: https://doi.org/10.5914/tropocean.v42i3.5767

Berlamont, J., Ockenden, M., Toorman, E. & Winterwerp, J. 1993. The characterization of cohesive sediment properties. *Coastal Engineering*, 21(1-3), 105-128. DOI: https://doi.org/10.1016/0378-3839(93)90047-C

Chen, M. S., Wartel, S., Eck, B. V. & Maldegem, D. V. 2005. Suspended matter in the Scheldt estuary. *Hydrobiologia*, 540, 79-104. DOI: https://doi.org/10.1007/s10750-004-7122-y

Garel, E., Pinto, L., Santos, A. & Ferreira, Ó. 2009. Tidal and river discharge forcing upon water and sediment

circulation at a rock-bound estuary (Guadiana estuary, Portugal). *Estuarine, Coastal and Shelf Science*, 84(2), 269-281. DOI: https://doi.org/10.1016/j.ecss.2009.07.002

Ghazali, M. E. B., Argo, Y., Kyotoh, H. & Adachi, Y. 2020. Effect of the concentration of NaCl and cylinder height on the sedimentation of flocculated suspension of Na-Montmorillonite in the semi-dilute regime. *Paddy and Water Environment*, 18, 309-316. DOI: https://doi.org/10.1007/s10333-019-00783-6

Gibbs, R. J. 1985. Estuarine flocs: their size, settling velocity and density. *Journal of Geophysical Research*, 90(C2), 3249-3251. DOI: https://doi.org/10.1029/jc090ic02p03249

Gibbs, R. J. 1986. Segregation of metals by coagulation in estuaries. *Marine Chemistry*, 18(2-4), 149-159. DOI: https://doi.org/10.1016/0304-4203(86)90004-6

IBGE (Instituto Brasileiro de Geografia e Estatística). 2017. *Indicadores de desenvolvimento sustentável – Edição 2017*. Available from: https://sidra.ibge.gov.br/pesquisa/ids/tabelas. Access on: 2022 Oct. 9.

IBGE (Instituto Brasileiro de Geografia e Estatística). 2021. *Base cartográfica contínua do Brasil, escala 1:250 000 – BC250. Versão 2021*. Available from: https://geoftp.ibge.gov.br/cartas_e_mapas/bases_cartograficas_continuas/bc250/versao2021/shapefile/. Access on: 2023 Jul. 20.

IOC, SCOR and IAPSO. 2010. The International Thermodynamic Equation of Seawater – 2010: Calculation and use of thermodynamic properties. *Intergovernmental Oceanographic Commission*, Manuals and Guides 56, Geneva, UNESCO.

INMET (Instituto Nacional de Meteorologia). 2017. *Precipitação pluviométrica estação D016 Ipojuca*. Available from: https://portal.inmet.gov.br/. Access on: 2022 Oct. 10.

Kösters, F., Grabemann, I. & Schubert, R. 2014. On SPM dynamics in the turbidity maximum zone of the Weser Estuary. *Die Küste*, 81(81), 393-408. Available from: https://hdl.handle.net/20.500.11970/101702. Access on: 2024 May. 16.

Krahl, E., Vowinckel, B., Ye, L., Hsu, T. J. & Manning, A. J. 2022. Impact of the salt concentration and biophysical cohesion on the settling behavior of bentonites. *Frontiers in Earth Science*, 10, 886006. DOI: https://doi.org/10.3389/feart.2022.886006

Kranenburg, C. 1994. The fractal structure of cohesive sediment aggregates. *Estuarine, Coastal and Shelf Science*, 39(6), 451-460. DOI: https://doi.org/10.1016/S0272-7714(06)80002-8

Krone, R. B. 1962. Flume studies of the transport of sediment in estuarial shoaling process (Final Report). Berkeley: Hydraulic Engineering Laboratory and Sanitary Engineering Research Laboratory, University of California.

Lee, B. J., Fettweis, M., Toorman, E. & Molz, F. J. 2012. Multimodality of a particle size distribution of cohesive suspended particulate matters in a coastal zone. *Journal of Geophysical Research: Oceans*, 117(C3). DOI: https://doi.org/10.1029/2011jc007552

Li, W., Zhang, W., Shan, B., Sun, B., Guo, X. & Li, Z. 2022. Risk assessment of heavy metals in suspended particulate matter in a typical urban river. *Environmental science and pollution research international*, 29(31), 46649-46664. DOI: https://doi.org/10.1007/s11356-022-18966-w

Lins, S. R. R. M. 2018. Propagação das marés salina e dinâmica no Rio Ipojuca-PE, Brasil (Mestrado em Oceanografia). Recife: Universidade Federal de Pernambuco.

Lins, S. R. R. M. & Medeiros, C. 2018. Propagação da maré salina em um estuário tropical estrangulado, Ipojuca, NE-Brasil. *Tropical Oceanography*, 46(1), 70-91. DOI: https://doi.org/10.5914/tropocean.v46i1.237251

Maggi, F. 2009. Biological flocculation of suspended particles in nutrient rich aqueous ecosystems. *Journal of Hydrology*, 376(1-2), 116-125. DOI: https://doi.org/10.1016/j.jhydrol.2009.07.040

Manning, A. J. & Bass, S. J. 2006. Variability in cohesive sediment settling fluxes: observations under different estuarine tidal conditions. *Marine Geology*, 235(1-4), 177-192. DOI: https://doi.org/10.1016/j.margeo.2006.10.013

Manning, A. J., Bass, S. J. & Dyer, K. R. 2007. Preliminary findings of a study of the upper reaches of the Tamar Estuary, UK, throughout a complete tidal cycle: Part II: In-situ floc spectra observations. in Estuarine and Coastal Fine Sediments Dynamics. *In*: Maa, J. P.-Y., Sanford, L. P. & Schoellhamer, D. H. (Ed.). *Proceedings in Marine Science* (v. 8, pp. 1-14). Amsterdam: Elsevier.

Manning, A. J. & Dyer, K. R. 2002. a comparison of floc properties observed during neap and spring tidal conditions. *In*: Winterwerp, J. C., Kranenburg, C. (Ed.). *Proceedings in marine science* (v. 5, pp. 233-250). Amsterdam: Elsevier.

Mikkelsen, O., Hill, P. & Milligan, T. 2006. Single-grain, microfloc and macrofloc volume variations observed with a LISST-100 and a digital floc camera. *Journal of Sea Research*, 55(2), 87-102. DOI: https://doi.org/10.1016/j.seares.2005.09.003

Millero, F. J. 2006. *Chemical oceanography*. 3rd. ed. Boca Raton, CRC Press.

Miranda, A. M. 2019. Condições ambientais do estuário do rio merepe (Pernambuco/BR): biomassa fitoplânctonica e parâmetros hidrológicos (Mestrado em Oceanografia). Recife: Universidade Federal de Pernambuco.

Miranda, L. B., Andutta, F. P., Kjerfve, B., & Castro, B. M. 2017. *Fundamentals estuarine physical oceanography*. Berlin, Springer.

Noriega, C., Santiago, M. F., Façanha, P., Silva Cunha, M. G., Silva, R., Flores Montes, M., Araujo, M., Costa, K. M., Eskinazi, E. & Neumann-Leitão, S. 2013. The instantaneous transport of inorganic and organic material in a highly polluted tropical estuary. *Marine and Freshwater Research*, 64(6), 562-572. DOI: https://doi.org/10.1071/MF12083

Oliveira, T. S., Xavier, D., Santos, L., França, E., Sanders, C., Passos, T. & Barcellos, R. 2020. Geochemical background indicators within a tropical estuarine system influenced by a port-industrial complex. *Marine Pollution Bulletin*, 161, 111794. DOI: https://doi.org/10.1016/j.marpolbul.2020.111794

PERNAMBUCO. Secretaria de Recursos Hídricos. 2010. Plano hidroambiental da bacia hidrográfica do rio Ipojuca: Tomo I – Diagnóstico hidroambiental – Volume

01/03 - Recursos Hídricos. Available from: https://www.apac.pe.gov.br/images/media/1569523666_PHA_Ipojuca_TOMO_I_VOL_1_Diagnostico_10.09.11.pdf. Access on: 2024 May. 16.

Schettini, C. A. F., Paiva, B. P., Batista, R. D. A. L., Oliveira Filho, J. C. D., Truccolo, E. C. 2016. Observation of an estuarine turbidity maximum in the highly impacted Capibaribe Estuary, Brazil. *Brazilian Journal of Oceanography*, 64(2), 185-190. DOI: https://doi.org/10.1590/S1679-87592016115006402

Seiphoori, A., Gunn, A., Kosgodagan Acharige, S., Arratia, P. E., & Jerolmack, D. J. 2021. Tuning sedimentation through surface charge and particle shape. *Geophysical Research Letters*, 48(7), e2020GL091251. DOI: https://doi.org/10.1029/2020gl091251

Strickland, J. D. H., Parsons, T. R. 1972. *A practical handbook of seawater analysis*. 2nd.ed. Ottawa, Queen's Printer.

Talley, L. D., Pickard, G. L., Emery, W. J. & Swift, J. H. 2011. *Descriptive physical oceanography: An introduction*. 6th. ed., Boston, Elsevier.

Telesh, I. V. & Khlebovich, V. V. 2010. Principal process within the estuarine salinity gradient: A review. *Marine Pollution Bulletin*, 61(4-6), 149-155, DOI: https://doi.org/10.1016/j.marpolbul.2010.02.008

Turner, A. & Millward, G. E. 2002. Suspended particles: their role in estuarine biogeochemical cycles. *Estuarine, Coastal and Shelf Science*, 55(6), 857-883, DOI: https://doi.org/10.1006/ecss.2002.1033

Varona, H. L., Noriega, C., Araujo, J., Lira, S., Araujo, M. & Hernandez, F. 2023. Plotting and statistical analysis for oceanographers, meteorologists and ecologists (mStatGraph). *Zenodo*, version (1.5). DOI: https://doi.org/10.5281/zenodo.8095883

Veiga, T. T., Santos, L. D. & Barcellos, R. L. 2021. Análise da dinâmica sedimentar espaço-temporal dos estuários do ipojuca e merepe (PE) com base nos componentes da fração arenosa (0,25mm e 0,50mm). *In*: Silva, C. D. D., Mota, D. A. (Org.). *A pesquisa em ciências biológicas: desafios atuais e perspectivas futuras* (pp. 1-18). 2nd. ed. Ponta Grossa: Atena.

Ye, L., Manning, A. J. & Hsu, T. J. 2020. Oil-mineral flocculation and settling velocity in saline water. *Water Research*, 173, 115569. DOI: https://doi.org/10.1016/j.watres.2020.115569

Ye, L., Manning, A. J., Holyoke, J., Penaloza-Giraldo, J. A. & Hsu, T. J. 2021. The role of biophysical stickiness on oil-mineral flocculation and settling in seawater. *Frontiers in Marine Science*, 8, 628827. DOI: https://doi.org/10.3389/fmars.2021.628827

Yuan, Y., Wei, H., Zhao, L. & Cao, Y. 2009. Implications of intermittent turbulent bursts for sediment resuspension in a coastal bottom boundary layer: A field study in the western Yellow Sea, China. *Marine Geology*, 263(1-4), 87-96. DOI: https://doi.org/10.1016/j.margeo.2009.03.023